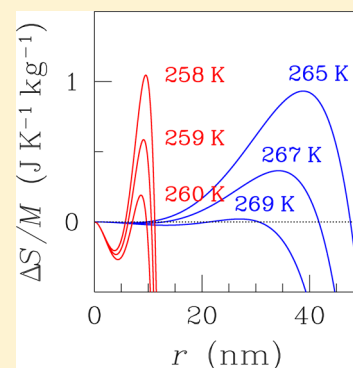


Spontaneous Freezing of Supercooled Water under Isochoric and Adiabatic Conditions

Santi Prestipino^{*,†,‡} and Paolo V. Giaquinta^{*,†}[†]Dipartimento di Fisica e di Scienze della Terra, Università degli Studi di Messina, Contrada Papardo, I-98166 Messina, Italy[‡]CNR-IPCF, Viale F. Stagno d'Alcontres 37, I-98158 Messina, Italy

ABSTRACT: The return of a supercooled liquid to equilibrium usually begins with a fast heating up of the sample which ends when the system reaches the equilibrium freezing temperature. At this stage, the system is still a microsegregated mixture of solid and liquid. Only later is solidification completed through the exchange of energy with the surroundings. Using the IAPWS-95 formulation, we investigate the adiabatic freezing of supercooled water in a closed and rigid vessel, i.e., under thermally and mechanically isolated conditions, which captures the initial stage of the decay of metastable water to equilibrium. To improve realism further, we also account for a fixed amount of foreign gas in the vessel. Under the simplifying assumption that the system is at equilibrium immediately after the nominal freezing temperature has been attained, we determine—as a function of undercooling and gas mole number—the final temperature and pressure of the system, the fraction of ice at equilibrium, and the entropy increase. Assuming a nonzero energy cost for the ice–water interface, we also show that, unless sufficiently undercooled, perfectly isolated pure-water droplets cannot start freezing in the bulk.



I. INTRODUCTION

When gently cooled below its equilibrium freezing point, liquid water becomes metastable, remaining in a state of apparent equilibrium until a favorable density fluctuation promotes the nucleation of ice. Once the first solid embryo has formed, ice growth proceeds so rapidly that crystallization of water initially occurs, to all practical purposes, adiabatically, i.e., as though water were thermally isolated from the environment.^{1–4} This phenomenon is well-known, especially in atmospheric science^{5,6} and metallurgy.^{7,8} It is accompanied with a steep temperature increase (*recalescence*),^{2,3} caused by the latent heat released during solidification, and is signaled by a sudden glowing of the sample or a change of color whatsoever. Freezing is nevertheless still partial after recalescence, requiring more time to be completed via standard heat transfer to the bath. The relative amount of water and ice at the end of the recalescence stage will clearly depend on the extent of undercooling as well as on the type of constraints applied to the system, e.g., whether its volume or pressure (besides the total mass) has been kept fixed.

Recalescence is an amazing phenomenon, since one might reasonably expect crystallization of a supercooled liquid to occur isothermally, with the energy reservoir grabbing all the heat generated by the formation of ice. Indeed, the entropy of the universe (system plus bath) is maximized in the stable crystal phase at the temperature of the bath. By contrast, what is often found is that kinetics influences the crystallization process in an essential way, bringing rapidly the system to the equilibrium freezing temperature before conduction of heat to the bath becomes effective. The route to equilibrium would be different if, for some reasons, crystal growth were much slower,

as in intrinsically anisotropic crystals. In this case the initial temperature rise would be milder and the system probably would not pass through intermediate states of two-phase coexistence at the freezing point.

Recently, Aliotta et al. discussed the adiabatic freezing of water under constant-pressure conditions.⁹ Upon modeling water by the IAPWS-95 formulation,¹⁰ they focused their attention on the behavior of volume at ambient pressure and found that the spontaneous freezing of water invariably results in an expansion. After reaching a maximum for a moderate undercooling, the expansion decreases on further cooling until it becomes negligible at a temperature close to the homogeneous-nucleation temperature, $T_H \approx 232$ K, which sets the ultimate threshold for water metastability. This behavior is different from that of other liquids, where the volume gap between the solid–liquid mixture and the metastable liquid varies monotonously with undercooling. Such a difference was traced back to the volumetric anomaly of water. Prestipino has also studied the adiabatic freezing of a mean-field fluid in a rigid vessel, also in the presence of a small amount of foreign gas in the container, and found a rather complex behavior in the properties (final temperature and pressure, solid fraction, and entropy increase) characterizing this type of irreversible freezing.¹¹

The method employed in ref 11 was entropy maximization. It assumes that at the end of recalescence the system is found in an *equilibrium* mixed state. Actually, as discussed at length in ref

Received: April 4, 2013

Revised: June 12, 2013

Published: June 25, 2013

11, the immediate outcome of recalescence is a uniform distribution of fine solid grains in the form of dendrites within the liquid (a so-called mushy zone), which is rich in interfacial energy. The conversion of the mushy zone into a full solid occurs by coarsening: it involves the slow assimilation of small grains by larger ones and requires some time during which the temperature of the system stays constant at the equilibrium freezing value. The point is that in the mushy zone the system is not yet at equilibrium, which implies that its state is not, strictly speaking, the maximum-entropy state. However, the huge (on the molecular scale) size of ice dendrites suggests that the amount of interfacial free energy in the mushy zone is macroscopically negligible. Hence, we reasonably expect that the maximum-entropy method does not miss the mark too much and that at least the general trends of the relevant system variables can be described within a purely thermodynamic framework.

In the present paper, the maximum-entropy method is applied to the spontaneous freezing of water under isolated conditions, stressing on the specificities arising from its anomalous thermodynamics. After describing the method in section II, we analyze the prominent features of the isochoric-adiabatic freezing of water in section III. These results are then exploited in section IV where we shall see to what extent the energy penalty associated with the ice–water interface does influence the spontaneous crystallization of water. Section V is devoted to concluding remarks.

II. METHOD

Experimentally, the clearest imprint of recalescence in water is a sudden increase of temperature which abruptly jumps (in a time which can be as low as a few hundredths of a second²) from the nucleation temperature to the equilibrium freezing temperature. During this time no significant amount of heat can flow to the bath and (partial) freezing then occurs adiabatically.

In Figure 1 we schematically illustrate, for the reader's convenience, the two steps in which a virtual experiment on adiabatic freezing is articulated under either isochoric or isobaric conditions, pretending that the outcome of the process is an equilibrium state. The system under focus here is a normal liquid, viz., the van der Waals fluid described by the theory developed in refs 14 and 15, which was the object of the study carried out by Prestipino in ref 11. Initially at point A, the liquid is subsequently cooled down to B (a metastable state), at temperature T_{in} . Next, heat exchange with the environment is impeded and the solid is made to nucleate, until point C (temperature T_{fin}) is reached. We see that in both the isochoric and isobaric cases the final equilibrium state C is a two-phase state. Under constant-volume conditions, the final temperature T_{fin} is intermediate between T_{in} and T_m (the melting/freezing temperature at a given pressure P_m), and the pressure is lower than P_m . The outcome of the same experiment on water can be anticipated on the basis of a construction analogous to that depicted in Figure 1, which is reported in Figure 2, where due account was taken of the change in relative position between liquid and solid on the isotherm for $T = T_m$ (point A now lies on the small-volume side of the tie line). As far as the other features of Figure 2 are concerned, we relied on the data reported in Table 19 of ref 12. At variance with Figure 1, the metastable liquid branch (long-dashed line) is shifted to pressures higher than P_m ; hence, when keeping the volume fixed, the final pressure P_{fin} will be larger than P_m .

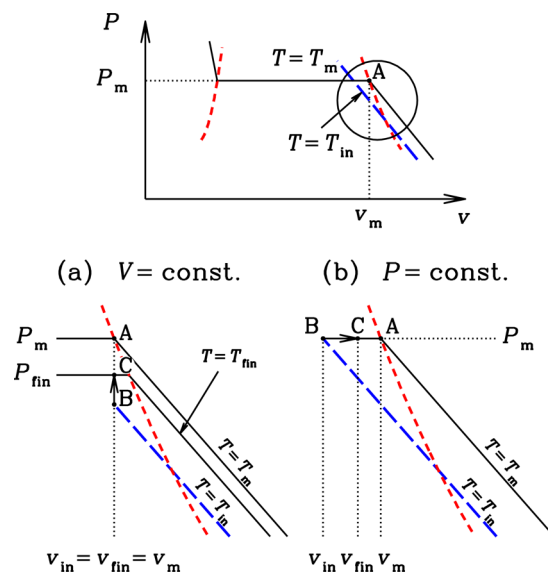


Figure 1. How adiabatic freezing occurs for the van der Waals liquid of ref 11 (schematic). Top: the isotherm at T_m on the volume–pressure plane (solid–liquid binodal, dashed red line; isotherm at T_{in} prolonged to the metastable region, long-dashed blue line). Bottom: a magnification of the (v,P) region involved in the process of adiabatic freezing (left, isochoric case; right, isobaric case). While A and C are equilibrium (respectively, homogeneous and heterogeneous) states, B corresponds to a one-phase (i.e., homogeneous) metastable condition.

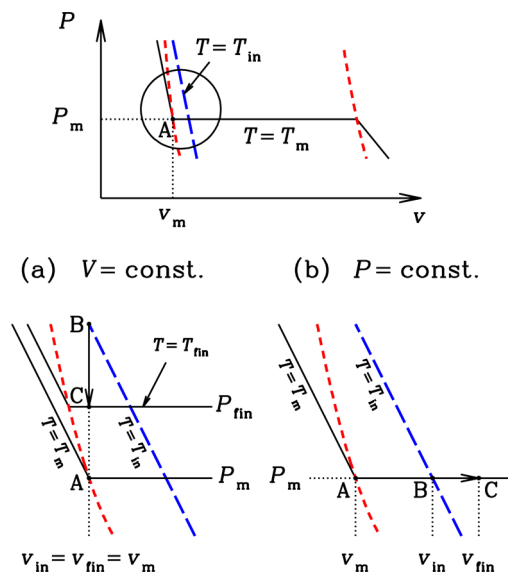


Figure 2. How adiabatic freezing occurs in water (same meaning and notation as in Figure 1).

We now describe the setup used for studying the adiabatic freezing of supercooled water in a rigid vessel. Consider a number N of water molecules which completely fill a closed rigid container of volume V . Water, initially in equilibrium at the temperature T_m , is then slowly cooled until the temperature T_{in} has been reached. At this point, if ice nucleation has not yet occurred, the pressure and energy of water (P_{in} and E_{in}) can be computed through the (mechanical and thermal) equations of state of the metastable branches. Now, imagine removing the contact with the thermostat and inducing, by any means, the irreversible decay of the system to equilibrium. Our aim is determining in which equilibrium state the system will

eventually settle down. With the caveats made above, this question may be answered by resorting to the maximum-entropy principle. Envisaging that part of the original water may remain liquid, we denote by E_l , V_l , and N_l the energy, volume, and particle number of the liquid fraction. By further assuming a weak coupling between the solid (s) and liquid (l) water phases, and taking the overall constraints into account, the total entropy reads

$$S_{\text{tot}} = S_l(E_l, V_l, N_l) + S_s(E_{\text{in}} - E_l, V - V_l, N - N_l) \quad (2.1)$$

where E_l , V_l , and N_l are internal variables to be determined. The three conditions for the maximum of (2.1) are tantamount to requiring the same temperature, pressure, and chemical potential for both phases. Hence we see that (unless $N_l = 0$ or N when S_{tot} is maximum) the final equilibrium state lies on the solid–liquid coexistence locus, as empirically observed.

As a matter of principle, in order to characterize the heterogeneous two-phase state resulting from the maximization of (2.1), one would need the entropy functions (fundamental relations) of water and ice. However, we can alternatively resort to a different thermodynamic potential for each phase, such as the Helmholtz or Gibbs potential, or to the knowledge of the equations of state, if available. This is actually the type of information provided by the IAPWS-95 formulation for the thermal properties of water¹⁰ and by its counterpart for hexagonal ice.¹² In particular, while the IAPWS-95 formulation provides the specific (i.e., per unit mass) Helmholtz free energy of liquid water, $f_l(T, \rho)$, as a function of temperature T and mass density ρ , it is the specific Gibbs free energy, $g_s(T, P)$, that is available for ordinary ice in ref 12.

We originally explored the possibility of seeking the maximum of eq 2.1 by the simulated-annealing method, which was the technique employed in ref 11 to analyze the adiabatic freezing of a mean-field fluid. However, in the present case this method did not work essentially because of the extreme sensitivity of water temperature and pressure to the small uncorrelated variations of energy and volume induced by the fake dynamics typical of the method. Hence, we implemented a different but equivalent procedure. Rather than maximizing the total entropy, we tried to solve the system of equations enforcing (i) the thermodynamic coexistence of water and ice in the final state, and (ii) the conservation laws of volume and energy. Specifically, the set of equations corresponding to the maximization of (2.1) reads

$$\begin{cases} P_l(T, \rho) = P \\ g_l(T, \rho) = g_s(T, P) \\ \frac{x_l}{\rho} + (1 - x_l)v_s(T, P) = v_{\text{tot}} \\ x_l e_l(T, \rho) + (1 - x_l)e_s(T, P) = e_{\text{in}} \end{cases} \quad (2.2)$$

where $x_l = N_l/N$ is the liquid fraction, $v_{\text{tot}} = V/M$ is the (constant) specific volume, M being the total mass, and $e_{\text{in}} = E_{\text{in}}/M$ is the specific energy of supercooled water at T_{in} . In addition, P_l , g_l , and e_l denote the pressure, specific Gibbs free energy, and specific energy of the liquid phase, respectively, while v_s and e_s represent the specific volume and energy of the solid phase. All such functions can be derived from $f_l(T, \rho)$ and $g_s(T, P)$ in an obvious way. Clearly, the unknown quantities in (2.2) are T , P , ρ , and x_l ; the existence and uniqueness of the

solution set are assured by the concavity of the entropies in (2.1).

While leaving the analysis of this solution to section III, we comment here on the method used to solve the nonlinear system (2.2) numerically and on the precision of the data extracted. The method of choice for this type of problems is the time-honored Newton–Raphson method,¹³ which also works in more than one dimension. This method makes use of an iterative scheme which usually converges if one starts not too far away from the target state; in our case the solution was obtained with the highest possible precision in 10–20 iteration steps. In fact, increasing more the number of steps does not reduce the error further, because of computer limitations in handling the real and complex numbers which enter the calculation. This notwithstanding, each unknown of (2.2) was typically obtained with 10 exact significant digits.

III. RESULTS

In this section we analyze the properties of the heterogeneous state attained by supercooled water at the end of its *isochoric–adiabatic* relaxation to equilibrium. Two different experimental situations are discussed, depending on whether water alone fills the given volume or there is, in addition, a fixed amount of gas (for instance, some air) in the container. These two cases are treated separately in the following.

A. Pure Water in a Rigid Vessel. Let us first quantitatively analyze the situation illustrated in Figure 2, panel (a). Initially, the water temperature and pressure are T_m and P_m , defining a point on the ice–water coexistence locus (the red dashed line in the figure). In this state, dubbed A in Figure 2, the specific volume is $v_m \equiv \rho_m^{-1}$, with ρ_m implicitly given by

$$P_l(T_m, \rho_m) = P_m \quad (3.1)$$

We just note that the initial volume coincides with the total volume, v_{tot} , since we assumed that water completely fills the container. This fixes the water mass M and the molecule number N for any assigned V . After cooling water down to $T_{\text{in}} < T_m$ (state B), its pressure and specific energy become equal to

$$P_{\text{in}} = P_l(T_{\text{in}}, \rho_m) \quad \text{and} \quad e_{\text{in}} = e_l(T_{\text{in}}, \rho_m) \quad (3.2)$$

With these starting conditions, the equilibrium state (C) eventually reached by the system after disconnecting the bath and inducing solid nucleation is the one yielding the maximum of (2.1) or, which amounts to the same thing, the one obeying the set of eqs 2.2.

We studied in detail the ambient-pressure case, $P_m = 101\,325$ Pa (for this pressure, $T_m = 273.152\,519$ K and $v_m = 1.000\,157 \times 10^{-3}$ m³ kg⁻¹). In Figure 3 the final values of the system temperature and pressure are reported as a function of T_{in} (red curves through crosses). As expected from Figure 2, we have $T_{\text{in}} < T_{\text{fin}} < T_m$ (i.e., water heats up during the transformation) and $P_{\text{fin}} > P_m$. Though water does not generally recover the original temperature after isochoric recalcence, nevertheless it should be considered that the pressure has increased as well. In fact, for any value of T_{in} , T_{fin} and P_{fin} are the coordinates of a point on the ice–water coexistence line. If water supersaturation is low or moderate, T_{in} can be hardly distinguished from T_m . The solid fraction in the equilibrium state is plotted in Figure 4: it steadily grows with the undercooling extent $T_m - T_{\text{in}}$, approaching 40% near T_{H} . Finally, Figure 5 reports the entropy increase in the transformation, which is larger the lower T_{in} .

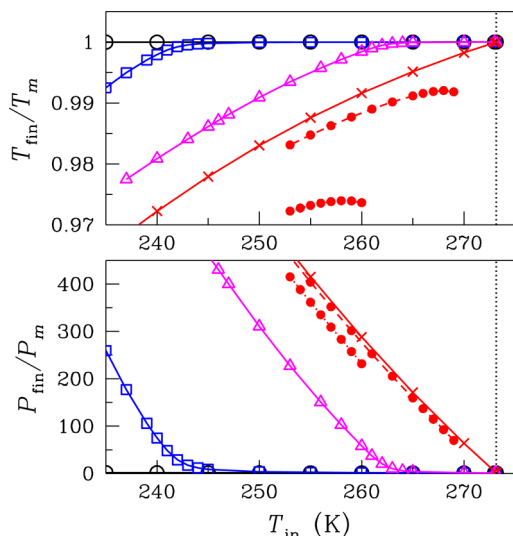


Figure 3. Adiabatic freezing of water under isochoric conditions: temperature and pressure in the final equilibrium state for $P_m = 101\,325\text{ Pa}$, plotted as a function of the supercooling temperature T_{in} . Data for a number of x_g values are collected together: 10^{-4} (black empty dots), 3×10^{-5} (blue squares), 10^{-5} (magenta triangles), and zero (i.e., no gas is present, red crosses). Data points are joined by line segments. The small, red full dots mark data relative to a finite system size for $x_g = 0$, when a cost is assumed for the ice–water interface ($N = 10^6$, dashed line; $N = 10^8$, dotted line). The vertical dotted line locates the equilibrium freezing temperature T_m .

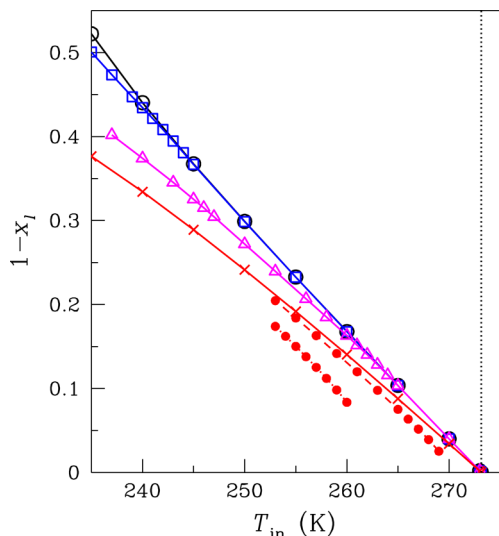


Figure 4. Adiabatic freezing of water under isochoric conditions: ice fraction in the final equilibrium state for $P_m = 101\,325\text{ Pa}$, plotted as a function of the supercooling temperature T_{in} (same notation as in Figure 3). The black curve practically coincides with that for isenthalpic freezing.⁹

B. Water with a Foreign Gas. Now suppose that water is prepared at T_m and P_m by exposure to a gaseous atmosphere, and that a small amount of gas gets trapped in the vessel. We then have water in equilibrium with a foreign (and, for simplicity, immiscible) gas in a container of fixed volume. To simplify the analysis further, the gas is treated as ideal and monatomic, and let x_g be the ratio of the gas mole number to that of water. The initial specific volume of the liquid, v_m , is still

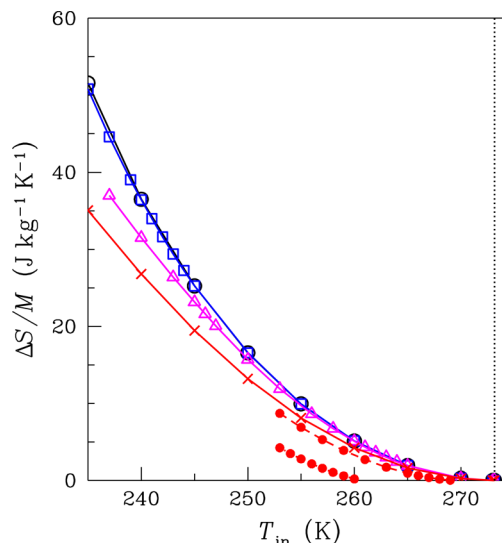


Figure 5. Adiabatic freezing of water under isochoric conditions: specific-entropy increase for $P_m = 101\,325\text{ Pa}$, plotted as a function of the supercooling temperature T_{in} (same notation as in Figures 3 and 4).

obtained by solving eq 3.1 but now we have $v_m < v_{tot}$. Precisely, the ratio of the total volume to water mass is

$$v_{tot} = v_m + \frac{x_g RT_m}{P_m} \tag{3.3}$$

where $R = 461.518\,05\text{ J kg}^{-1}\text{ K}^{-1}$ is the specific gas constant, namely the ratio of the universal gas constant to water molar mass. As before, we imagine that water and gas are cooled very slowly until a temperature T_{in} is reached. At this point, the specific volume v_{in} of water is determined by minimizing the total Helmholtz free energy, $F/M = f_l(T_{in}, v_{in}^{-1}) + x_g f_{id}(T_{in}, \rho_g)$ with $\rho_g \equiv n_g/V_g = x_g/(v_{tot} - v_{in})$ (f_{id} is the ideal-gas Helmholtz free energy per mole divided by the water molar mass). This leads immediately to the equation

$$P_l(T_{in}, v_{in}^{-1}) = \frac{x_g RT_{in}}{v_{tot} - v_{in}} \tag{3.4}$$

which prescribes the same pressure for water and gas. Equation 3.4 was solved by the Newton–Raphson method (for the smallest x_g considered, the bisection method proved superior for deep undercoolings).

After removing the bath, we imagine to induce ice nucleation by, e.g., a mechanical shock, and wait for the system to reach equilibrium. The state eventually attained is the one that maximizes the total entropy

$$\begin{aligned} \frac{S_{tot}}{M} = & x_l s_l(e_l, v_l) + (1 - x_l) s_s(e_s, v_s) \\ & + x_g s_{id} \left(\frac{e_{in} - x_l e_l - (1 - x_l) e_s}{x_g}, \frac{v_{tot} - x_l v_l - (1 - x_l) v_s}{x_g} \right) \end{aligned} \tag{3.5}$$

where $e_{in} = e_l(T_{in}, v_{in}^{-1}) + (3/2)x_g RT_{in}$ (note that s_l and s_s are entropies per unit mass, whereas s_{id} is the ideal-gas entropy per mole divided by the water molar mass). If one is able to find the maximum of S_{tot} , the ensuing values of e_l, v_l, x_l, e_s, v_s will provide a complete description of the equilibrium state. Upon noting that the five conditions for the maximum of (3.5) are equivalent

to requiring the same temperature and pressure for water, ice, and the foreign gas at equilibrium, as well as equal chemical potentials for the liquid and solid fractions in the ice–water mixture, a different solution method is possible and actually preferable (for the same reasons exposed in section II). Calling v_g the molar volume of the gas divided by the water molar mass, the resulting set of equations analogous to (2.2) is

$$\begin{cases} P_l(T, \rho) = P \\ g_l(T, \rho) = g_s(T, P) \\ \frac{x_l}{\rho} + (1 - x_l)v_g(T, P) + x_g v_g = v_{\text{tot}} \\ x_l e_l(T, \rho) + (1 - x_l)e_s(T, P) + (3/2)x_g RT \\ = e_{\text{in}} \\ P v_g = RT \end{cases} \quad (3.6)$$

which is again solved by the Newton–Raphson method.

In order to characterize adiabatic freezing, useful quantities to be monitored as a function of T_{in} are the following: the temperature and pressure of the ice–water mixture at equilibrium, T_{fin} and P_{fin} ; the specific volume of the mixture, $v_{\text{mix}} = x_l v_l + (1 - x_l)v_s$, as compared to v_{in} ; and the entropy of the mixture, in comparison with the entropy of the supercooled liquid. We examined a few x_g values in the range from 10^{-5} to 10^{-4} for $P_m = 101\,325$ Pa. In Figure 3 we report data for T_{fin} and P_{fin} as a function of undercooling. We see that the gas, when present in an appreciable amount, acts as a pressure moderator; in particular, P_{fin} is extremely close to P_m down to a threshold temperature \tilde{T} , which is pushed down and down upon increasing x_g , until, beyond a certain x_g value, \tilde{T} drops below T_H . In this case, practically the same results of isobaric–adiabatic freezing are recovered. Near \tilde{T} we observe a change of slope in all curves, related to an abrupt crossover in the gas pressure at T_{in} (i.e., the right-hand side of eq 3.4) from small to very large values, i.e., only above \tilde{T} the gas volume at T_{in} is a significant portion of the total volume (see Figure 6). Hence, the gas provides a way to continuously interpolate between the isochoric and isobaric cases of adiabatic freezing of pure water.

In Figure 4, the equilibrium ice fraction is plotted for various values of x_g . Compared to $x_g = 0$, the amount of ice formed at equilibrium is larger, the more so the larger x_g . For the same values of x_g , Figure 5 reports the entropy difference between the mixture and the supercooled liquid at T_{in} . This difference increases with undercooling. Finally, in Figure 6 we plot the volume of the ice–water mixture in comparison with the initial volume of supercooled water. Upon cooling, a clear changeover of v_{mix} is seen to occur for $T \simeq \tilde{T}$. From this temperature downward, the gas is strongly compressed and its volume reduces more rapidly but v_{mix} always keeps larger than v_{in} , which means that adiabatic freezing always occurs in water with a system expansion. It would be interesting to see whether this volume behavior is confirmed experimentally (by, e.g., looking at the free-surface level before and after recalescence). This would also offer a way to check to what extent the system state after recalescence can be described as an equilibrium one.

IV. FINITE-SIZE EFFECTS IN THE FORMATION OF ICE

So far, our analysis of water freezing under isolated supercooled conditions has made use of a simplifying assumption: namely, we neglected any surface effect. We shall now see that, even

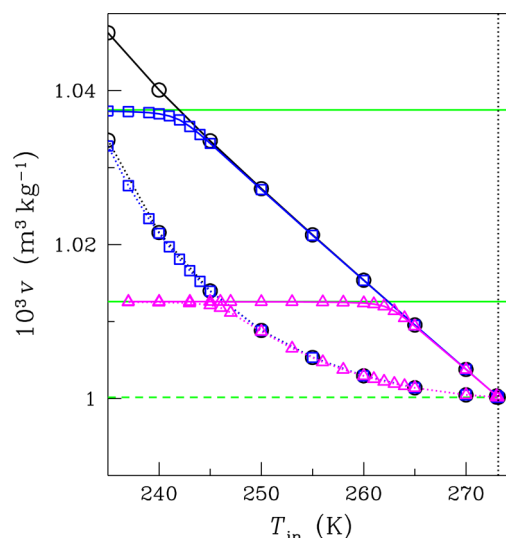


Figure 6. Adiabatic freezing of water under isochoric conditions: initial (i.e., $T = T_{\text{in}}$, dotted line) and final volume (full line) for $P_m = 101\,325$ Pa, plotted as a function of the supercooling temperature T_{in} (same notation as in Figures 3, 4, and 5). Data for a number of x_g values are shown: 10^{-4} (black empty dots), 3×10^{-5} (blue squares), and 10^{-5} (magenta triangles). Data points are joined by line segments. The horizontal dashed line marks the value of v_m . The two horizontal green full lines locate the value of v_{tot} for $x_g = 3 \times 10^{-5}$ (above) and 10^{-5} (below). The black curve is practically coincident with that for isenthalpic freezing.⁹

overlooking the porous structure of the mushy zone as well as any interfacial effect at the boundary between water and its container, just the simple consideration of a spherical ice–water interface unveils a fundamental limitation of the adiabatic-freezing scenario as depicted above. Indeed, this is what was found for the van der Waals liquid,¹¹ where, under perfect isolation, no freezing can initiate in the bulk if undercooling is too small. The same analysis is repeated here for supercooled water.

Our reasoning, which is similar to a proof per absurdum, goes as follows. Let us assume that the outcome of water freezing below T_m is a stable mixture of water and ice. We make the further hypothesis that homogeneous (rather than heterogeneous) nucleation superintends the onset of freezing. By modeling the ice fraction as a spherical (not necessarily tiny) mass, we assign a constant free energy γ to its surface (for instance, $\gamma = 2.8 \times 10^{-2}$ J m⁻², which is the value of the ice–water interface free energy at normal freezing conditions⁵). While this scenario is certainly too simplified, since it overlooks the dependence of the interface free energy on the droplet radius r (see, e.g., ref 16) as well as on the surface orientation,¹⁷ it would be nonetheless sufficient to grasp the essence of the phenomenon. With the above settings, the entropy of a mass M of water hosting a spherical ice droplet of mass M_s is written, in terms of the specific ice values of energy and volume, as¹¹

$$\begin{aligned} S_{\text{tot}}(e_s, v_s, M_s; E_{\text{in}}, V, M) \\ = (M - M_s)s_l(e_l, v_l) + M_s s_s(e_s, v_s) \end{aligned} \quad (4.1)$$

where E_{in} is the total energy (we note that, for a constant γ , the entropy and the particle number attached to the interface are both zero by the Gibbs adsorption equation¹¹). In eq 4.1, the specific energy and volume of the liquid fraction are respectively given by

$$e_1 = \frac{E_1}{M_1} = \frac{E_{\text{in}} - M_s e_s - (36\pi)^{1/3} \gamma (M_s v_s)^{2/3}}{M - M_s} \quad \text{and}$$

$$v_1 = \frac{V_1}{M_1} = \frac{V - M_s v_s}{M - M_s} \quad (4.2)$$

For $\gamma = 0$, the maximum of (4.1) clearly coincides with that of (2.1) for the same T_{in} .

The values of the internal variables e_s , v_s , M_s in a stationary (possibly unstable) equilibrium state are obtained by equating the three partial derivatives of S_{tot} to zero. It is then a simple matter to show that these conditions are equivalent to

$$T_s(e_s, v_s) = T_l(e_1, v_1)$$

$$P_s(e_s, v_s) = P_l(e_1, v_1) + \frac{2\gamma}{r}$$

$$\mu_s(e_s, v_s) = \mu_l(e_1, v_1) \quad (4.3)$$

where again $r = (3M_s v_s / (4\pi))^{1/3}$. Hence, any cluster of ice in equilibrium with liquid water should have the same temperature and chemical potential as the melt, while the two pressures are different and related by the Laplace equation. In particular, eqs 4.3 would hold for the cluster of ice in the heterogeneous state associated with the absolute maximum of S_{tot} . In order to determine this state, we have solved numerically a set of equations analogous to (2.2), namely

$$\begin{cases} P_l(T, \rho) = P - K_1(1 - x_1)^{-1/3} v_s(T, P)^{-1/3} \\ g_l(T, \rho) = g_s(T, P) \\ \frac{x_1}{\rho} + (1 - x_1) v_s(T, P) = v_{\text{tot}} \\ x_1 e_1(T, \rho) + (1 - x_1) e_s(T, P) + K_2 \\ \quad (1 - x_1)^{2/3} v_s(T, P)^{2/3} \\ = e_{\text{in}} \end{cases} \quad (4.4)$$

where

$$K_1 = \left(\frac{32\pi}{3M} \right)^{1/3} \gamma \quad \text{and} \quad K_2 = \left(\frac{36\pi}{M} \right)^{1/3} \gamma \quad (4.5)$$

To be sure that the correct solution of eqs 4.4 is being picked out, the starting point of the Newton–Raphson iteration is chosen as the solution of (2.2) for the same T_{in} . The interface free energy is then gradually switched on, and the entropy maximum point recalculated, until γ is led back to the right value.

However, for low enough supersaturation, the maximum of the total entropy is invariably found for $M_s = 0$. In order to clarify what is going on, we should look at the graph of the function $\Delta S = S_{\text{tot}}(e_s, v_s, M_s; E_{\text{in}}, V, M) - M_s (E_{\text{in}}/M, V/M)$, which represents the entropic advantage of the two-phase system over the supercooled liquid. To simplify it further, ΔS is projected onto the one-dimensional subspace where e_s and v_s take the same values as in the point of the absolute maximum of S_{tot} . We are thus left with a function of M_s only, or equivalently of the radius r , which is reported in Figure 7 for two small values of N (10^6 and 10^8) and a few undercooling temperatures (note that the functional form of ΔS is not strictly needed to plot the graph on Figure 7; in fact, the values of T_{fin} and P_{fin} for ice, as determined by solving eqs 4.4, suffice). A glance at Figure 7 immediately reveals the existence of a positive maximum of ΔS

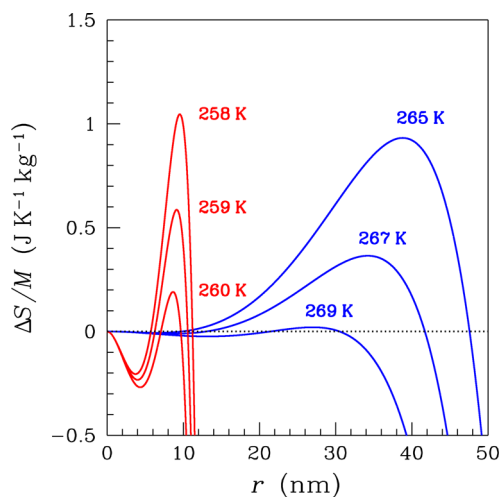


Figure 7. Specific entropy difference between the droplet–liquid mixture at T_{fin} and the original metastable liquid at T_{in} , for $P_{\text{in}} = 101\,325$ Pa, plotted as a function of the droplet radius r . Two values of N are considered, 10^6 (red curves, left) and 10^8 (blue curves, right), over a range of T_{in} values (reported alongside).

for a nonzero M_s value, corresponding to a two-phase equilibrium state. However, a satellite maximum also exists at the origin, which is separated from the former one by an entropic “barrier” (the valley between the two peaks), and when the extent of supercooling becomes sufficiently low, the absolute maximum of ΔS jumps to $M_s = 0$. Hence, (i) ice formation is thermally activated (i.e., the crossing of the entropic barrier requires a favorable density fluctuation), and (ii) for any fixed value of N , there is an undercooling threshold (negligible for macroscopic N) that should be overcome in order that solidification may occur. Figure 8 displays the

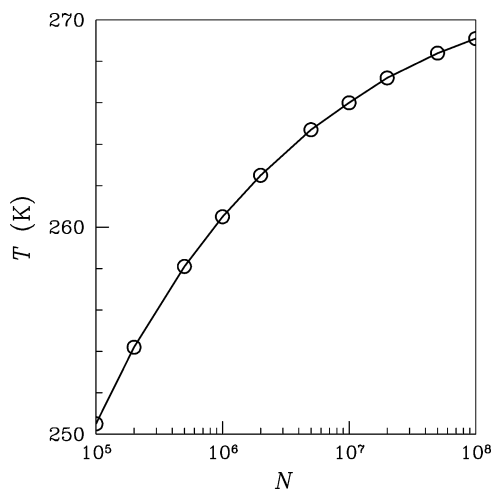


Figure 8. Lower supercooling threshold for partial freezing of an isolated liquid sample in the bulk, plotted as a function of the particle number.

minimum supercooling threshold for a number of N values. Beyond this threshold, the assumption of a rapid yet partial solidification of water, which is at the heart of the present calculation, should be rejected—since no ice fraction is found in the equilibrium state—and the onset of solidification would necessarily occur at the surface of the system in contact with the bath. Upon reducing the supersaturation even further, the

relative maximum for $M_s > 0$ disappears and no tiny piece of ice, even metastable, can form. We note that a scenario similar to the one described above has recently been reported for the canonical-ensemble description of liquid nucleation from the vapor.¹⁸

In Figures 3, 4, and 5, some properties of the heterogeneous equilibrium state for a nonzero γ are reported. We first note that, compared to a costless interface, the final equilibrium temperature is lower by an amount which roughly scales as r^{-1} (Figure 3, top panel). The depression of T_{fin} is a clear manifestation of the Gibbs–Thomson effect, which refers to the observation that small crystals are in equilibrium with their own melt at a lower temperature than large crystals. It is also evident from the figure that the variation of r with supercooling leads to a notable nonmonotonous dependence of the equilibrium temperature on T_{in} . Similar reductions with respect to $\gamma = 0$ values are found in the final pressure (Figure 3, bottom panel), in the ice fraction (Figure 4), and in the entropy increase ΔS (Figure 5). Actually, we are not aware of any experimental or numerical-simulation studies where the above predictions can be tested in detail.

Summing up, the aim of the above calculation was to check whether the assumption of adiabaticity in the spontaneous freezing of supercooled water can survive the inclusion of the interface-energy contribution. A necessary condition for this is a positive maximum of ΔS which, however, only appears beyond a certain N -dependent undercooling threshold that is negligible in the large-size limit. This implies that a small amount of water should be cooled sufficiently deep in order that freezing may start in the bulk; otherwise, homogeneous ice nucleation is obstructed and freezing proceeds directly from the system boundaries.

V. CONCLUSIONS

The spontaneous freezing of a supercooled liquid occurs adiabatically whenever solid growth is sufficiently rapid, as in the case of, e.g., water. In this circumstance, the energy released during solidification does not reach the thermostat but is almost completely used in the heating up of the system, whose temperature raises quickly until the equilibrium freezing temperature is attained. Only later will crystallization proceed by heat transfer to the bath.

In this paper, we have studied the isochoric–adiabatic freezing of supercooled water, as modeled by the IAPWS-95 formulation;¹⁰ for ice properties we employed the scheme of ref 12. We have characterized the thermodynamic state of the two-phase equilibrium emerging from the decay of the metastable state in two different experimental setups, i.e., in the presence as well as in the absence of a spectator gas. We have thus found that the spontaneous freezing of water always occurs with a system expansion, as under constant-pressure conditions,⁹ and that by tuning the amount of gas present in the container one is able to interpolate between the isochoric and isobaric cases of adiabatic freezing. The hidden assumption behind our calculations is that the state of the system emerging from recalescence is an equilibrium one. However, the outcome of adiabatic freezing is usually a mushy zone, which only slowly evolves to equilibrium. Anyway, considering that solid dendrites are huge on the molecular scale, we argue that at least the overall trends of the relevant system properties with supercooling should be largely insensitive to the late system relaxation dynamics and could thus be predicted by the maximum-entropy method.

In order to see whether surface effects can play any role in the irreversible freezing of small water samples under isolation, we have then included the energy cost of the ice–water interface in the treatment, while assuming no role for heterogeneous nucleation. We have thus shown that, under isolated conditions, a minimum supersaturation is needed in order that freezing may start in the bulk.

■ AUTHOR INFORMATION

Corresponding Author

*E-mail: sprestipino@unime.it (S.P.); paolo.giaquinta@unime.it (P.V.G.)

Notes

The authors declare no competing financial interest.

■ ACKNOWLEDGMENTS

We gratefully acknowledge useful discussions with Franco Aliotta, Rosina C. Ponterio, Franz Saija, and Cirino Vasi.

■ REFERENCES

- (1) Macklin, W. C.; Payne, G. S. A Theoretical Study of the Ice Accretion Process. *Q. J. R. Meteorol. Soc.* **1967**, *93*, 195–213.
- (2) Hindmarsh, J. P.; Wilson, D. I.; Johns, M. L. Using Magnetic Resonance to Validate Predictions of the Solid Fraction Formed during Recalescence of Freezing Drops. *Int. J. Heat Mass Transfer* **2005**, *48*, 1017–1021.
- (3) Tellinghuisen, J. Vapor Pressure Plus: An Experiment for Studying Phase Equilibria in Water, with Observation of Supercooling, Spontaneous Freezing, and the Triple Point. *J. Chem. Educ.* **2010**, *87*, 619–622.
- (4) Debenedetti, P. G. *Metastable Liquids*; Princeton University Press: Princeton, NJ, 1996.
- (5) Pruppacher, H. R.; Klett, J. *Microphysics of Clouds and Precipitation*; Springer: New York, 1997.
- (6) Kostinski, A.; Cantrell, W. Entropic Aspects of Supercooled Droplet Freezing. *J. Atmos. Sci.* **2008**, *65*, 2961–2971.
- (7) Glicksman, M. E. *Principles of Solidification*; Springer, Berlin, 2010; Chapter 2.
- (8) Bendert, J. C.; Gangopadhyay, A. K.; Mauro, N. A.; Kelton, K. F. Volume Expansion Measurements in Metallic Liquids and Their Relation to Fragility and Glass Forming Ability: An Energy Landscape Interpretation. *Phys. Rev. Lett.* **2012**, *109*, 185901.
- (9) Aliotta, F.; Giaquinta, P. V.; Pochylski, M.; Ponterio, R. C.; Prestipino, S.; Saija, F.; Vasi, C. Volume Crossover in Deeply Supercooled Water Adiabatically Freezing under Isobaric Conditions. *J. Chem. Phys.* **2013**, *138*, 184504.
- (10) Wagner, W.; Pruss, A. The IAPWS Formulation 1995 for the Thermodynamic Properties of Ordinary Water Substance for General and Scientific Use. *J. Phys. Chem. Ref. Data* **2002**, *31*, 387–535.
- (11) Prestipino, S. A Maximum-Entropy Approach to the Adiabatic Freezing of a Supercooled Liquid. *J. Chem. Phys.* **2013**, *138*, 164501.
- (12) Feistel, R.; Wagner, W. A New Equation of State for H₂O Ice Ih. *J. Phys. Chem. Ref. Data* **2006**, *35*, 1021–1047.
- (13) See e.g.: Scott, L. R. *Numerical Analysis*; Princeton University Press: Princeton, NJ, 2011.
- (14) Daanoun, A.; Tejero, C. F.; Baus, M. van der Waals Theory for Solids. *Phys. Rev. E* **1994**, *50*, 2913–2924.
- (15) Coussaert, T.; Baus, M. Making a (Colloidal) Liquid: A van der Waals Approach. *Phys. Rev. E* **1995**, *52*, 862–869.
- (16) Prestipino, S.; Laio, A.; Tosatti, E. Systematic Improvement of Classical Nucleation Theory. *Phys. Rev. Lett.* **2012**, *108*, 225701.
- (17) Prestipino, S.; Laio, A.; Tosatti, E. A Fingerprint of Surface-Tension Anisotropy in the Free-Energy Cost of Nucleation. *J. Chem. Phys.* **2013**, *138*, 064508.
- (18) Calecki, D.; Lederer, D.; Roulet, B.; Diu, B.; Guthmann, C. Fixed Volume versus Fixed Pressure Liquid-Vapor Transition. *Am. J. Phys.* **2010**, *78*, 1316–1322.